



**HAL**  
open science

## Reduction of the non-uniform illumination using nonlocal variational models for document image analysis

Fatim Zahra Aït Bella, Mohammed El Rhabi, Abdelilah Hakim, Amine  
Laghrib

► **To cite this version:**

Fatim Zahra Aït Bella, Mohammed El Rhabi, Abdelilah Hakim, Amine Laghrib. Reduction of the non-uniform illumination using nonlocal variational models for document image analysis. Journal of The Franklin Institute, inPress, 10.1016/j.jfranklin.2018.08.012 . hal-01874941

**HAL Id: hal-01874941**

**<https://enpc.hal.science/hal-01874941>**

Submitted on 15 Sep 2018

**HAL** is a multi-disciplinary open access archive for the deposit and dissemination of scientific research documents, whether they are published or not. The documents may come from teaching and research institutions in France or abroad, or from public or private research centers.

L'archive ouverte pluridisciplinaire **HAL**, est destinée au dépôt et à la diffusion de documents scientifiques de niveau recherche, publiés ou non, émanant des établissements d'enseignement et de recherche français ou étrangers, des laboratoires publics ou privés.

# Reflectance and illumination decomposition using nonlocal models

Ait Bella Fatim Zahra<sup>a,\*</sup>, Mohammed El Rhabi<sup>b</sup>, Abdelilah Hakim<sup>a</sup>,  
Amine Laghrib<sup>c</sup>

<sup>a</sup>*Cadi Ayyad University, LAMAI FST Marrakech, Morocco;*

<sup>b</sup>*Applied Mathematics and Computer Science department, Ecole des Ponts ParisTech (ENPC), Paris, France.*

<sup>c</sup>*LMA FST Béni-Mellal, Sultan Moulay Slimane University, Morocco*

\* *Corresponding author : aitbella.fatimzehrae@gmail.com*

---

## Abstract

In this paper, we investigate two new reflectance and illumination decomposition models based on a nonlocal partial differential equation (PDE) applied to text images. Taking into consideration the higher regularity level of the illumination compared to the reflectance, we propose a nonlocal PDE which deals with repetitive structures and textures that characterize the text image much better compared to the classical local PDEs. The aim of this approach is to use the repetitive features of the reflectance to efficiently extract it from the nonuniform illumination. This idea is motivated by extending the range of application of the nonlocal operators to such problem. Numerical experiments on both grayscale and color text images show the performance and strength of the proposed nonlocal PDE.

*Keywords:* Nonlocal operators, Partial differential equation, Text image, Viscosity solutions theory

---

## 1. Introduction

In image analysis, reflectance and illumination decomposition is a basic process which aims to enhance the image by reducing or removing the effects of the nonuniform illumination. This technique, which is named the Retinex problem, represents a necessary pretreatment step in a wide range of image processing applications.

The image decomposition is considered as an ill-posed problem since it consists in extracting two unknown parts from an observed image. The Retinex theory was first proposed by Land and McCann in [27] to address and improve the quality of an image when the lighting conditions are not satisfactory [26, 33]. The main idea of this theory is to consider the human visual system as a color perception where we can define the reflectance associated to a field in which both illumination and reflectance are unknown. Indeed, for a given scene, our visual system detects and sees the same color even if the illuminations conditions vary. This explains that the color of the objects is considered invariant in spite of illumination transformations.

The main goal of Retinex theory is to decompose a given image  $u$  into two components represented by the following model:

$$u(x, y) = I(x, y)R(x, y). \quad (1)$$

The model assumes that the observed image  $u$  is the product of two main components [18], namely the illumination  $I$  and the reflectance image  $R$ . According to the single-scale Retinex algorithm, the reflectance is estimated as described by the following equation:

$$\log(R_i(x, y)) = \log(u_i(x, y)) - \log(F(x, y) * u_i(x, y)), \quad (2)$$

where  $*$  is the convolution operator,  $R_i$  is the reflectance image on the  $i^{th}$  channel and  $F$  is a Gaussian filter defined by

$$F(x, y) = C \exp^{-\left(\frac{x^2+y^2}{\sigma^2}\right)}, \quad (3)$$

where  $C$  is a normalization factor.

This single-scale Retinex formula is extended to a multi-scale version in [24, 40]. This approach is pursued and introduced by Brelstaff [4] and Horn [19], who proposed a Retinex algorithm based on Poisson equation. In 2003, Kimmel and Elad proposed a variational Retinex approach [25]; to form a penalty functional, the authors call into question some hypotheses about the illumination image: the illumination is spatially smooth, it is close to the intensity image  $u$  and  $I \geq u$ , moreover they assume that the illumination continues smoothly as a constant beyond the image boundaries. Other approaches are presented using the same principle. First, Ma and Osher have introduced a total variation regularized formulation and an efficient algorithm based on the split Bregman method, then, they took advantage of

the nonlocal total variation to enhance the resulting images [31]. Further, Chen et al have used a TV-L1 based variational Retinex approach [31]. More recently, Liang and Zhang suggested a reflectance and illumination decomposition model for the Retinex problem using a convex variational model based on high-order total variation and  $L^1$  decomposition [28]. This method can effectively decompose the gradient component of images into salient edges and slightly smoother illumination field.

Another famous method to correct the non-uniform illumination is the Homomorphic filtering. This approach was introduced by Oppenheim et Al [37], the main idea of this technique is to decompose the image into high and low frequencies components, as a result the enhanced image is obtained through a high-pass filter in order to remove the illumination component. The improvement is then achieved by the simultaneous compression of the intensity range and the contrast enhancement. This method gave reasonable results and have been used in many applications [12, 10, 17].

On the other hand and precisely in document-image processing, many approaches are proposed to enhance the quality of a document-image. This generates a text which is easier to read in order to extract it thereafter using an optical character recognition (OCR). In 1995, W. Jiang has investigated a thresholding and enhancement method [22] which consists of converting text images of low spatial resolution to bi-level images of higher spatial resolution. In the same principle, a simple algorithm based on empirical mode decomposition was proposed in [39] to improve the illumination problem for document-image. However, there are several other methods specified for document-image enhancement with different degrees of success, see for examples [41, 7, 23, 11].

The main objective of this paper is to provide an improved nonlocal approach to remove the shadow from a document-image. Nonlocal operators have received much attention in the past decade. Such operators were first introduced by Gilboa and Osher [16]. The purpose of their paper is the use of nonlocal operators to treat signal and image processing by adopting the so called nonlocal PDE. Convinced by the effectiveness and efficiency of the nonlocal operators in dealing better with image textures, we introduce two new nonlocal PDEs to enhance the text quality and make it more meaningful and expressive for the human eye. These two nonlocal PDEs take into consideration the fact that illumination varies more smoothly than reflectance and also consider the effect of the illumination on image features such as texture. This can help the model to be able to take into account the surroundings of

the object much better compared to some classical approaches.

The paper is organized as follows. In section 2, we will focus on introducing a local model which we aim to extend to the nonlocal case, we recall some essential and basic definitions and properties of viscosity solutions theory and we prove the existence of a unique solution of this problem, section 3 deals with the formulation of the new nonlocal models, in section 4, two algorithms are presented to solve the proposed nonlocal models, and in order to assess the validity of the proposed approach we will present some numerical tests in section 5, finally we shall sum up by a conclusion where we will outline the big points covered in the paper.

## 2. Problem Formulation

We consider a document-image  $u$  acquired by a camera phone. In general, many degradation factors are involved by this acquisition, such as : noise, non-uniform illumination and motion blur. Note that in this paper, the blur is not considered. In fact, the studied model is based on the separation of the two components of the image: the illumination  $I$  and the reflectance  $R$

$$u(x, y) = I(x, y)R(x, y) + n(x, y), \quad (4)$$

where  $n$  is the noise. As discussed above, we firstly neglect the noise and we apply the logarithm function, we obtain then the additive model

$$\log(u(x, y)) = \log(I(x, y)) + \log(R(x, y)). \quad (5)$$

Our aim is to consider a decomposition approach to recover the illumination  $I$  by estimating the term "  $\log I$ ". In particular, we focus on extracting illumination  $I$  using a nonlocal PDE in a well posed functional framework. Our proposed model is considered as a nonlocal version of the PDE proposed in [32]. The idea behind this choice is related to recently developed nonlocal operators [16]. Therefore, in the following, we recall the studied PDE and also we present some theoretical results. The local PDE is defined by

$$\begin{cases} \frac{\partial u}{\partial t} &= \max(0, \Delta u) & \text{in } \Omega \times (0, T) \\ \frac{\partial u}{\partial n} &= 0 & \text{on } \partial\Omega \times (0, T) \\ u(\cdot, 0) &= u_0 & \text{in } \Omega \end{cases} \quad (6)$$

where  $\Omega$  is a bounded open subset of  $\mathbb{R}^2$  and  $\Delta$  is the Laplacian operator defined by

$$\Delta u = \frac{\partial^2 u}{\partial x^2} + \frac{\partial^2 u}{\partial y^2}. \quad (7)$$

The method proposed in [32] which aims to resolve the equation (6) supposes that the document-image  $u$  has been acquired by a cameraphone. The authors consider two problem types; namely: image distortions and noise. Especially, they address the so-called non uniform illumination or variations of brightness. In image processing applications, a shadow is considered as a region with low lightness and high gradient contours. There are in fact two kinds of shadows, the own shadow and the shadows arising from the acquisition process. Own shadow occurs when the light hits a surface with a slope change. Otherwise, the brightness of pixels decreases when the angle of incidence deviates from the normal of the surface. While the brightness reaches its minimum value in the case when the incident light and the surface normal are orthogonal. A shadow always occurs when the light source is obscured by an object before the light reflection on the surface. Taking into account that the image contains only text, the background is preponderant compared to the text in the image (or there is much more background than text in the image). Also knowing that the intensity of the background is superior to the intensity of the text (light background on dark writing), it is easy to approximate the background. Indeed, intuitively, in order to estimate the background, we replace each pixel by considering the maximum mean of its neighboring pixels and we iterate that is to say if  $u_{ij}^n$  represents the intensity of the image in the spatial location  $(i, j)$  at the  $n^{th}$  iteration, we get:

$$u_{ij}^{n+1} = \max(u_{ij}^n, \hat{u}_{ij}^{1,n}, \hat{u}_{ij}^{2,n}, \hat{u}_{ij}^{3,n}, \hat{u}_{ij}^{4,n}), \quad (8)$$

where  $\hat{u}^k$  is the mean calculated in the  $k^{th}$  direction using the neighboring pixels (see Fig.1). By subtracting  $u_{ij}^n$  from both sides of the equation (8), the discrete derivatives in all directions appear and we get the discretized version of the equation:

$$\frac{\partial u}{\partial t} = \frac{1}{2} \max \left( 0, \frac{\partial^2 u}{\partial x^2}, \frac{\partial^2 u}{\partial y^2}, \frac{\partial^2 u}{\partial x^2} + \frac{\partial^2 u}{\partial y^2} + 2 \frac{\partial^2 u}{\partial x \partial y}, \frac{\partial^2 u}{\partial x^2} + \frac{\partial^2 u}{\partial y^2} - 2 \frac{\partial^2 u}{\partial x \partial y} \right) \quad (9)$$

in a similar way, considering only the horizontal and vertical directions, one can easily get the equation (6).

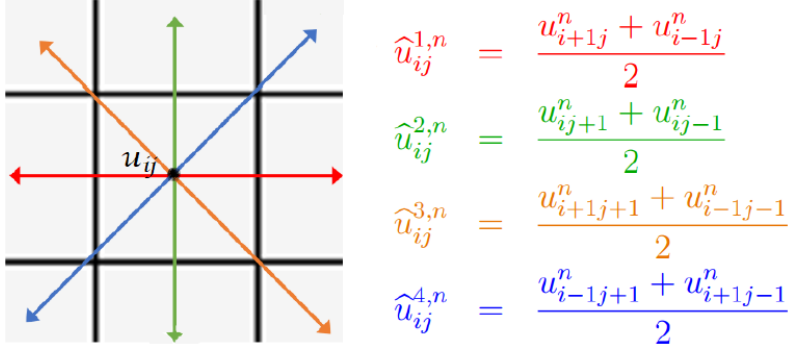


Figure 1: The mean at the neighboring pixels of the image  $u$ .

Realeyes 3D company and M. El Rhabi have successfully implemented this equation as an embedded application for document scanning in more than 150 million smartphones in the world from 2006 to 2010. In this paper, as a first step, we choose a simplified form of this equation which coincides with equation (6). Then, we rewrite (9) in its non local formulation which we analyse.

The equation (6) has demonstrated its robustness in the extraction of the variable luminance and it has given quite satisfactory results (see [32]). However, the theoretical aspect of this equation has not been investigated, which left a lack of information on the behavior and the existence of the solution. As a first contribution in this work, we are interested in the theoretical side of this model. The complexity to show the existence of a solution to the equation (6) comes from the fact that we cannot say anything about the maximum of two operators. We intend here to find a continuous viscosity solution of (6). We first give a brief overview of some essential notions of the viscosity solutions theory [8, 15, 2].

The theory deals with some partial differential equations of the form :

$$F(x, u, \nabla u, \nabla^2 u) = 0, \quad (10)$$

where  $x$  is defined in an open subset  $\Omega$  of  $\mathbb{R}^n$ .  $F$  is a real-valued function on  $D = \Omega \times \mathbb{R} \times \mathbb{R}^n \times S^n$ , where  $S^n$  stands for the set of symmetric  $n \times n$  matrices,  $u$  denotes the real-valued unknown function on  $\Omega$ ,  $\nabla u$  and  $\nabla^2 u$  designate respectively, the gradient and the Hessian matrix of  $u$ .

The function  $F$  is called degenerate elliptic if it verifies the following inequality:

$$F(x, r, p, X) \leq F(x, r, p, Y) \quad \text{for } Y \leq X, \quad (11)$$

where  $Y \leq X$  signifies:

$$\langle X\xi, \xi \rangle \leq \langle Y\xi, \xi \rangle \quad \forall \xi \in \mathbb{R}^n. \quad (12)$$

If  $F$  is degenerate elliptic, we can say that it is proper if:

$$F(x, r, p, X) \leq F(x, s, p, Y) \quad \text{for } Y \leq X, \quad r \leq s. \quad (13)$$

Let  $u : E \rightarrow \mathbb{R} \cup \{\pm\infty\}$ , where  $E$  is a set of a metric space. The upper semi-continuous envelope  $u^*$ , and the lower semi-continuous envelope  $u_*$  of  $u$  are given respectively by

$$\begin{aligned} u^*(y) &= \limsup_{r \rightarrow 0} \{u(z) / z \in B(y, r) \cap E\}, \\ u_*(y) &= \liminf_{r \rightarrow 0} \{u(z) / z \in B(y, r) \cap E\}, \end{aligned}$$

where  $B(y, r)$  is a closed ball of radius  $r$  centred at  $y \in \bar{E}$ .

**Definition 1.** [15] Let  $\Omega$  be an open set in  $\mathbb{R}^n$  and  $T > 0$  a fixed time parameter.

Let  $F : \bar{\Omega} \times [0, T] \times \mathbb{R} \times \mathbb{R}^n \times S^n \rightarrow \mathbb{R}$  be a continuous function.

Let  $U$  be an open set in  $\Omega \times ]0, T[$ .

A function  $u : U \rightarrow \mathbb{R} \cup \{-\infty\}$  is a viscosity sub-solution of

$$\frac{\partial u}{\partial t} + F(x, t, u, \nabla u, \nabla^2 u) = 0, \quad (14)$$

in  $U$  if:

- $u^*(x, t) < \infty$  for  $(x, t) \in U$ .
- If  $(\varphi, \hat{x}, \hat{t}) \in \mathcal{C}^2(U) \times U$  satisfies

$$\max_U (u^* - \varphi) = (u^* - \varphi)(\hat{x}, \hat{t}). \quad (15)$$

then

$$\frac{\partial \varphi}{\partial t}(\hat{x}, \hat{t}) + F(\hat{x}, \hat{t}, u^*(\hat{x}, \hat{t}), \nabla \varphi(\hat{x}, \hat{t}), \nabla^2 \varphi(\hat{x}, \hat{t})) \leq 0. \quad (16)$$

**Definition 2.** [15] A function  $u : U \rightarrow \mathbb{R} \cup \{+\infty\}$  is a viscosity supersolution of (14) in  $U$ , if

- $u_*(x, t) > -\infty$  for  $(x, t) \in U$ .
- If  $(\varphi, \hat{x}, \hat{t}) \in \mathcal{C}^2(U) \times U$  satisfies

$$\min_U (u_* - \varphi) = (u_* - \varphi)(\hat{x}, \hat{t}), \quad (17)$$

then

$$\frac{\partial \varphi}{\partial t}(\hat{x}, \hat{t}) + F(\hat{x}, \hat{t}, u_*(\hat{x}, \hat{t}), \nabla \varphi(\hat{x}, \hat{t}), \nabla^2 \varphi(\hat{x}, \hat{t})) \geq 0 \quad (18)$$



**Definition 3.** [15] A continuous function  $u : U \rightarrow \mathbb{R} \cup \{\pm\infty\}$  is a viscosity solution of (14) in  $U$ , if it is both a viscosity subsolution and a viscosity supersolution of (14) in  $U$ .

We apply theorem 3.1 in [21] to get the following existence result:

**Theorem 1.** Let  $\Omega$  be a regular bounded open subset of  $\mathbb{R}^2$ . Let  $u \in USC([0, T[ \times \bar{\Omega})$  (upper semicontinuous), and  $v \in LSC([0, T[ \times \bar{\Omega})$  (lower semicontinuous), be, respectively, a viscosity sub and a supersolutions of

$$\frac{\partial u}{\partial t} - \max(0, \Delta u) = 0 \text{ in } \Omega \times ]0, T[ \quad (19)$$

and

$$\frac{\partial u}{\partial n} = 0 \quad \text{on } \partial\Omega \times ]0, T[ \quad (20)$$

If

$$u(x, 0) \leq v(x, 0) \quad \text{for } x \in \bar{\Omega} \quad (21)$$

then

$$u \leq v \quad \text{in } ]0, T[ \times \bar{\Omega}$$

Moreover, for each  $u_0 \in C(\bar{\Omega})$ , there exists a unique continuous viscosity solution  $u \in C([0, T[ \times \bar{\Omega})$  of (6).

**Proof**

First of all, we use the following decomposition of the max operator

$$\max(0, \Delta u) = H(\Delta u)\Delta u \quad (22)$$

where  $H$  is the Heaviside step function, defined by

$$\forall x \in \mathbb{R}, \quad H(x) = \begin{cases} 0 & \text{if } x < 0 \\ 1 & \text{if } x \geq 0 \end{cases} \quad (23)$$

Afterwards, we consider the function  $F : S^n \rightarrow ]-\infty, 0]$ , given by:

$$F(X) = -H(\text{trace}(X))\text{trace}(X). \quad (24)$$

According to the theorem 2.1 in [21], we have to prove that  $F$  is continuous and there exists a continuous function  $w : [0, \infty[ \rightarrow [0, \infty[$  satisfying  $w(0) = 0$ , such that if  $X, Y \in S^n$  and  $\mu_1, \mu_2 \in [0, \infty[$  satisfy

$$\begin{pmatrix} X & 0 \\ 0 & Y \end{pmatrix} \leq \mu_1 \begin{pmatrix} I & -I \\ -I & I \end{pmatrix} + \mu_2 \begin{pmatrix} I & 0 \\ 0 & I \end{pmatrix}, \quad (25)$$

then

$$F(X) - F(-Y) \geq -w(\mu_2). \quad (26)$$

We start then by the continuity which is evident, since the functions

$$\begin{aligned} f &: S^n \rightarrow \mathbb{R} \\ X &\mapsto \text{trace}(X) \end{aligned}$$

and

$$\begin{aligned} g &: \mathbb{R} \rightarrow ]-\infty, 0] \\ x &\mapsto -H(x)x \end{aligned}$$

are continuous. Now, we suppose that there exist  $\mu_1, \mu_2 \in [0, \infty[$  such that the inequality (25) is satisfied.

We multiply both sides of the inequality by the matrix  $\begin{pmatrix} I & I \\ I & I \end{pmatrix}$ ,

We then apply the trace operator, we obtain

$$\text{trace}(X) + \text{trace}(Y) \leq 2n\mu_2. \quad (27)$$

Afterwards, taking the decreasing function  $g(x) = -H(x)x$  yields

$$\begin{aligned} -H(2n\mu_2)2n\mu_2 &= -2n\mu_2 \\ &\leq -H(\text{trace}(X) + \text{trace}(Y))(\text{trace}(X) + \text{trace}(Y)) \\ &\leq \frac{1}{2}(-\text{trace}(X) - \text{trace}(Y) - |\text{trace}(X) + \text{trace}(Y)|) \\ &\leq \frac{1}{2}(-\text{trace}(X) - \text{trace}(Y) - |\text{trace}(X)| + |\text{trace}(Y)|) \\ &= F(X) - F(-Y). \end{aligned} \quad (28)$$

Finally, we take  $w(r) = 2nr$  which satisfies  $w(0) = 0$ .

According to the theorem 2.1 and theorem 3.1 in [21], the results of comparison and existence of a unique viscosity solution is reached.  $\square$

As demonstrated in [32], the used PDE (6) has given good results, but does not preserve well the fine details of the text. This can be interpreted

by the use of a local image reconstruction algorithm using observations in a neighborhood of a pixel of the interest. However, in some cases the selection of the neighborhood plays a major role in the quality of the image reconstruction. This led us to think to the nonlocal version of the equation (6). In the nonlocal techniques, algorithms analyse data in a larger neighborhood and collect the observations from the whole image, searching similar features, which is much better and accurate. Indeed, the nonlocal methods, compared to local methods, are more effective, in particular to restore fine and repetitive structures of the image, which is the case of document-images. These approaches which are called also patch methods, allow to characterize a pixel with a vector of attributes wider than the intensity or color value of the pixel only. A patch representing a pixel is considered as a square sub-image of the original image, centered at this pixel, of a selected width. The patch-based methods were first used in the texture synthesis [9]. Also, they were then used for filtering and restoring degraded image [5]. More recently, it have also been extended to inpainting problems [16]. In the following section, we introduce the proposed nonlocal model to extract the illumination  $I$  and we give a result of the existence and uniqueness of the solution.

### 3. The proposed nonlocal approaches

In this section, we introduce the two nonlocal PDEs and we give some theoretical results. We start by the definition of the first model.

#### 3.1. The first model

As discussed above, we propose a new model for document-image enhancing. Therefore, we intend to obtain a new nonlocal generalization of the local model presented in [32]. As a preliminary, we recall some definitions of nonlocal operators introduced by Gilboa and Osher [16].

Let  $\Omega \subset \mathbb{R}^2$ , and  $u : \Omega \rightarrow \mathbb{R}$  denote a real function.

The nonlocal gradient  $\nabla_w u(x)$  at  $x \in \Omega$  is defined as the vector of all partial derivatives  $\nabla_w u(x, \cdot)$ :

$$(\nabla_w u)(x, y) := (u(y) - u(x))\sqrt{w(x, y)}, \quad y \in \Omega, \quad (29)$$

where  $w$  stands for a symmetric and positive weight function.

For any pair of  $v_1, v_2 : \Omega \times \Omega \rightarrow \mathbb{R}$ , one defines

$$(v_1 \cdot v_2)(x) := \int_{\Omega} v_1(x, y)v_2(x, y)dy, \quad (30)$$

and the inner product

$$\langle v_1, v_2 \rangle := \int_{\Omega \times \Omega} v_1(x, y)v_2(x, y)dx dy. \quad (31)$$

With the above definition of inner product and nonlocal gradient, the nonlocal divergence of  $v : \Omega \times \Omega \rightarrow \mathbb{R}$  at  $x$  is defined as the negative adjoint of the nonlocal gradient:

$$(\operatorname{div}_w v)(x) := \int_{\Omega} (v(x, y) - v(y, x))\sqrt{w(x, y)}dy. \quad (32)$$

The nonlocal Laplacian of  $u : \Omega \rightarrow \mathbb{R}$  is then defined by:

$$(\Delta_w u)(x) := \frac{1}{2} \operatorname{div}_w((\nabla_w u)(x)) = \int_{\Omega} (u(y) - u(x))w(x, y)dy. \quad (33)$$

At this point, we can use these operators to introduce the proposed nonlocal PDE. Indeed, to estimate the variable illumination we introduce the following model:

$$\begin{cases} \frac{\partial u}{\partial t} = \max(0, \Delta_w u) & \text{in } \Omega \times [0, \infty[ \\ u(\cdot, 0) = u_0 & \text{in } \Omega \end{cases} \quad (34)$$

where  $u_0 \in L^2(\Omega)$  is a given degraded image. This problem is seen as an evolution equation with homogeneous Neumann boundary condition, which mean that when integrating in  $\Omega$ , we suppose that there is no flux across the boundary. Before resolving this PDE, we have to check the existence and uniqueness of the solution. We are now ready to state our main result

**Theorem 2.** *Let  $\Omega$  be a bounded open subset of  $\mathbb{R}^2$ . Then, the problem (34) admits a unique generalized global solution  $u \in \mathcal{C}([0, +\infty[; L^2(\Omega))$ .*

### Proof

Basically, we use the following decomposition of the max operator

$$\max(0, \Delta_w u) = \frac{1}{2}(\Delta_w u + |\Delta_w u|) \quad (35)$$

According to the definition of  $\Delta_w u$  and (35), we consider the bounded linear operator  $A$  given by

$$Au = \frac{1}{2}u(\cdot) \int_{\Omega} w(\cdot, y)dy. \quad (36)$$

The operator  $A$  is the infinitesimal generator of  $S(t) = e^{-tA}$ ,  $t \geq 0$ . On the other hand, the function:

$$f(u) = \frac{1}{2} \left( \int_{\Omega} u(y) w(\cdot, y) dy + \left| \int_{\Omega} (u(y) - u) w(\cdot, y) dy \right| \right) \quad (37)$$

is an M-Lipschitz continuous function, indeed  $\forall t > 0, \forall u, v \in L^2(\Omega)$ :

$$\begin{aligned} |f(u(t)) - f(v(t))|_{L^2(\Omega)} &\leq \|\Omega\| \|w\|_{L^\infty(\Omega \times \Omega)} (2 \|u - v\|_{L^1(\Omega)} + \|u - v\|_{L^2(\Omega)}) \\ &\leq \|\Omega\| \|w\|_{L^\infty(\Omega \times \Omega)} (2c + 1) \|u - v\|_{L^2(\Omega)} \end{aligned}$$

We introduce now the operator  $\psi$  given by:

$$\psi(u)(t) = S(t)u_0 + \int_0^t S(t-s)f(u(s))ds. \quad (38)$$

We shall show that  $\psi$  maps

$$E_\alpha = \{u \in \mathcal{C}([0, \infty[; L^2(\Omega)); |u|_{E_\alpha} < +\infty\}$$

equipped with the norm  $|u|_{E_\alpha} = \sup_t (e^{-\alpha t} |u(t)|_{L^2(\Omega)})$  into  $E_\alpha \forall \alpha > 0$ .

$E_\alpha$  is a complete space since it is a closed subset of  $\mathcal{C}([0, \infty[; L^2(\Omega))$ . we have

$$\begin{aligned} \forall t > 0, |\psi(u)(t)|_{L^2(\Omega)} &\leq |S(t)u_0|_{L^2(\Omega)} + \int_0^t \|S(t-s)\|_{\mathcal{L}(L^2(\Omega))} |f(u(s))|_{L^2(\Omega)} ds \\ &\leq |u_0|_{L^2(\Omega)} + \int_0^t |f(u(s))|_{L^2(\Omega)} ds \\ &\leq |u_0|_{L^2(\Omega)} + \int_0^t (|f(u(s)) - f(0)|_{L^2(\Omega)} + |f(0)|_{L^2(\Omega)}) ds \\ &\leq |u_0|_{L^2(\Omega)} + \int_0^t (M |u(s)|_{L^2(\Omega)} + C) ds. \end{aligned} \quad (39)$$

We multiply this last inequality by  $e^{-\alpha t}$  for  $t > 0$ . We obtain then :

$$\begin{aligned} \forall t > 0; e^{-\alpha t} |\psi(u)(t)|_{L^2(\Omega)} &\leq e^{-\alpha t} |u_0|_{L^2(\Omega)} + \int_0^t e^{-\alpha(t-s)} e^{-\alpha s} (M |u(s)|_{L^2(\Omega)} + C) ds \\ &\leq e^{-\alpha t} |u_0|_{L^2(\Omega)} \\ &\quad + M \sup_s (e^{-\alpha s} |u(s)|_{L^2(\Omega)}) \int_0^t e^{-\alpha(t-s)} ds + tC e^{-\alpha t} \\ &\leq |u_0|_{L^2(\Omega)} + \frac{1}{\alpha} M |u|_{E_\alpha} + C \sup_t (te^{-\alpha t}). \end{aligned} \quad (40)$$

Thus

$$\sup_{t>0} e^{-\alpha t} \|\psi(u)(t)\|_{L^2(\Omega)} < +\infty. \quad (41)$$

Therefore, we can define the function  $\psi$  as follows,  $\forall \alpha > 0$ :

$$\psi : E_\alpha \rightarrow E_\alpha$$

Now, we shall show that  $\psi$  is a contraction on  $E_\alpha$ : let  $u, v \in E_\alpha$  and  $t \geq 0$ , we have

$$\begin{aligned} \|\psi(u)(t) - \psi(v)(t)\|_{L^2(\Omega)} &= \left\| \int_0^t S(t-s)(f(u(s)) - f(v(s))) ds \right\|_{L^2(\Omega)} \\ &\leq M \int_0^t \|u(s) - v(s)\|_{L^2(\Omega)} ds. \end{aligned} \quad (42)$$

Hence

$$\forall t > 0, \quad e^{-\alpha t} \|\psi(u)(t) - \psi(v)(t)\|_{L^2(\Omega)} \leq \frac{M}{\alpha} \|u - v\|_{E_\alpha}. \quad (43)$$

This shows that the operator  $\psi$  is a contraction on  $E_\alpha$  if  $\alpha > M$ . Consequently, using the Banach fixed-point theorem [38] we deduce the existence of a unique fixed point of  $\psi$  in  $E_\alpha$ . This fixed point is the desired solution of the integral equation

$$u(t) = S(t)u_0 + \int_0^t S(t-s)f(u(s))ds \quad (44)$$

Which concludes the proof.  $\square$

### 3.2. The second model

We conclude this section by presenting another new nonlocal model using the nonlocal second derivatives. The main idea is to take into consideration the second order opposite derivatives instead of considering only the nonlocal Laplacian operator. In fact, we consider all the directions presented in Fig.1. This technique is inspired by the benefits of considering the different directions in a document-image to handle the complexity of text texture in the degraded image. In [16], Gilboa and Osher derived also the nonlocal second

order derivatives. Let  $u : \Omega \subset \mathbb{R}^2 \rightarrow \mathbb{R}$  be a function, and  $w : \Omega \times \Omega \rightarrow \mathbb{R}$  be a nonnegative and symmetric weight function, then for  $i = 1, 2$ :

$$\begin{aligned} \left( \frac{\partial^2 u}{\partial x_i^2} \right)_w &:= \nabla_w(\nabla_w(u) \cdot \nabla_w(x_i)) \cdot \nabla_w(x_i) \\ &= \nabla_w \left( \int_{\Omega} (u(y) - u(x)) w(x, y) (y_i - x_i) dy \right) \cdot \nabla_w(x_i) \end{aligned} \quad (45)$$

Following the same idea, we establish the following text enhancement model to extract the variable illumination from an image:

$$\begin{cases} \frac{\partial u}{\partial t} &= \max(0, \left(\frac{\partial^2 u}{\partial x_1^2}\right)_w, \left(\frac{\partial^2 u}{\partial x_2^2}\right)_w, \left(\frac{\partial^2 u}{\partial x_1^2}\right)_w + \left(\frac{\partial^2 u}{\partial x_2^2}\right)_w + 2\left(\frac{\partial^2 u}{\partial x_1 x_2}\right)_w, \left(\frac{\partial^2 u}{\partial x_1^2}\right)_w \\ &+ \left(\frac{\partial^2 u}{\partial x_2^2}\right)_w - 2\left(\frac{\partial^2 u}{\partial x_1 x_2}\right)_w) \text{ in } \Omega \times (0, T) \\ u(, 0) &= u_0 \quad \text{in } \Omega \end{cases} \quad (46)$$

In the next section, we describe briefly the proposed algorithms for solving the problems (34) and (46).

#### 4. Numerical implementation

We begin by defining the weight function to measure the similarities between the pixels which is generally based on a gray level intensity vector comparison between two pixels. A pixel is characterized by its neighboring pixels belonging to a neighborhood window centered at its position, and the weight is calculated using the difference between these patches. Indeed, several forms of weight functions can be used [43, 6]. Note that the choice of the weight function is crucial for the success of non-local methods. In this paper, we propose a non-negative real-valued and symmetric weight function depending on the spatial distance only:

$$w(x, y) = \exp\left(\frac{-|x - y|^2}{h}\right), \quad (47)$$

where  $u : \Omega \rightarrow \mathbb{R}$  is a given image,  $\Omega \in \mathbb{R}^2$  is a bounded open domain and  $h$  is a positive parameter.

Before introducing the two proposed algorithms, we consider the following discretization of the nonlocal Laplacian operator:

$$\Delta_w(u_i) = \sum_{j \in N_i} (u_j - u_i) w_{i,j} \quad j \in N_i, \quad (48)$$

where  $u_i$  is the value of a pixel  $i$  ( $1 \leq i \leq N$ ),  $N_i = \{j : |i - j| \leq r\}$  denotes the neighbors set of the pixel  $i$ , and  $w_{i,j}$  is the discretized form of the weight function :

$$w_{i,j} = \exp\left(\frac{-|i - j|^2}{h}\right). \quad (49)$$

To discretize the non-local second derivative operators, we give the discretized version of the non-local gradient:

$$\nabla_w(u_i) = (u_j - u_i)\sqrt{w_{i,j}} \quad j \in N_i, \quad (50)$$

and the discrete inner product for vectors is given by:

$$(v_1 \cdot v_2)_i := \sum_{j \in N_i} (v_{1,i,j} v_{2,i,j}) \quad j \in N_i. \quad (51)$$

The second order discretized nonlocal derivatives are given by:

$$(u_i)''_{k,l} = \nabla_w(\nabla_w(u_i) \cdot \nabla_w(i_k)) \cdot \nabla_w(i_l) \quad k, l \in \{1, 2\}, \quad (52)$$

where  $i_k$  is the  $k^{\text{th}}$  component of the pixel  $i$  and

$$\nabla_w(i_k)(j) = (j_k - i_k)\sqrt{w_{i,j}} \quad j \in N_i. \quad (53)$$

Now we are ready to implement the two proposed algorithms based on the discretization form of non-local operators given above. We give firstly the algorithm 1 for solving the problem (34) as follows:

---

Algorithm 1 for solving (34)

---

**Input :** The acquired image  $u$

**initialization :** We set  $I^0 = \log(u + 1)$  and choose  $dt > 0$ ,  $h > 0$

**Compute :**

$$I_i^{n+1} = I_i^n + dt \max(0, \Delta_w(I_i^n)) \quad i = 1, \dots, N$$

**Output :** The illumination  $I$ .

The reflectance  $R = \exp(\log(u + 1) - I)$

---

In the same way, the algorithm 2 is given for resolving the second model in (46) using the nonlocal second order derivatives instead of the nonlocal Laplacian operator:

---

Algorithm 2 for solving (46)

---

**Input :** The acquired image  $u$

**initialization :** We set  $I^0 = \log(u + 1)$  and choose  $dt > 0$ ,  $h > 0$

**Compute :**

$$I_i^{n+1} = I_i^n + dt \max(0, (I_i^n)''_{1,1}, (I_i^n)''_{2,2}, (I_i^n)''_{1,1} + (I_i^n)''_{2,2} + 2(I_i^n)''_{1,2}, \\ (I_i^n)''_{1,1} + (I_i^n)''_{2,2} - 2(I_i^n)''_{1,2}) \quad i = 1, \dots, N$$

**Output :** The reflectance image  $R = \exp(\log(u + 1) - I)$

---



## 5. Numerical results

This section is devoted to the experimental part to test the two proposed nonlocal algorithms. Our aim is to confirm the performance and the robustness of the nonlocal models compared to some local methods in extracting the reflectance of a document-image.

The considered images in the reflectance and illumination decomposition problem are assumed to be degraded images acquired under variable illumination. For that, we consider six document-images taken in low light conditions. The first four images are given in grayscale level while the two last ones are color document-images. We compare the two nonlocal algorithms with some available methods in the literature, namely the variational method proposed in [25] (called Variational Retinex), the multiscale Retinex approach [40] (MSRetinex) and two Retinex methods based on partial differential equations proposed in [34, 29] (Screened Poisson Equation) and (PDE Retinex) respectively.

Figs. 2-7 show the obtained results using the two proposed algorithms compared to the other methods. Throughout this section, for the proposed methods, we set  $h = 80$ , while the numerical results by the variational Retinex method are reported with  $\alpha = 0.0001$  and  $\beta = 0.1$ , we set the threshold parameter  $t = 4$  for the PDE-Retinex model, and  $\lambda = 0.0001$  the tradeoff parameter for the Screened Poisson Equation, while the parameters in the implementation of Multiscale Retinex are chosen as follows:

parameter	N	$\sigma_1$	$\sigma_2$	$\sigma_3$	$\alpha$	$\beta$	$w_n$	G	b
value	3	15	80	250	125	46	1/3	192	-30

Note that for the first four grayscale images, we consider also a binarization step to show better the estimated text. In the following, we investigate a quantitative comparison in terms of OCR using the restored images in the previous tests apart the handwriting images. Optical Character Recognition tools are efficiently used to convert an image file or PDF file into editable and searchable text format. However, there are many limitations of OCR that can lead to inaccurate or missing text, the OCR engines fail usually to take into account blurry documents, colored paper, mathematical formulas or handwritten text.

The table 1 compares the character recognition rates for the grayscale images

using three different types of OCR tools, the "Abbyy FineReader 12"<sup>1</sup>, the software "Tesseract"<sup>2</sup> and the free web-based optical character recognition software "OnlineOCR.net"<sup>3</sup> that return a text with the best confidence rating. The rate "%" is obtained by a careful calculation of the correct characters from the OCR output. The table proves, as might be expected, and identically to the visual comparison in the six different examples, that the two non-local approaches can better recover the degraded text compared to the other approaches, providing then promising numerical results. In comparison, considering the greyscale images, we established that the two proposed methods can reduce the effects of the nonuniform illumination to a greater degree than the other methods. The model based on the nonlocal second derivatives seemed to enhance better color document-images than the first nonlocal model. Our two nonlocal methods, while different, performed comparably at estimating the reflectance part.

---

<sup>1</sup>[https://en.wikipedia.org/wiki/ABBYY\\_FineReader](https://en.wikipedia.org/wiki/ABBYY_FineReader)

<sup>2</sup>[https://en.wikipedia.org/wiki/Tesseract\\_\(software\)](https://en.wikipedia.org/wiki/Tesseract_(software))

<sup>3</sup><https://www.onlineocr.net/>

**Proposition 12** Si  $A$  et  $2D - A$  sont symétriques définies positives alors la méthode de Jacobi converge pour tout choix de  $x^{(0)}$ .

(a)

**Proposition 12** Si  $A$  et  $2D - A$  sont symétriques définies positives alors la méthode de Jacobi converge pour tout choix de  $x^{(0)}$ .

(b)

**Proposition 12** Si  $A$  et  $2D - A$  sont symétriques définies positives alors la méthode de Jacobi converge pour tout choix de  $x^{(0)}$ .

(c)

**Proposition 12** Si  $A$  et  $2D - A$  sont symétriques définies positives alors la méthode de Jacobi converge pour tout choix de  $x^{(0)}$ .

(d)

**Proposition 12** Si  $A$  et  $2D - A$  sont symétriques définies positives alors la méthode de Jacobi converge pour tout choix de  $x^{(0)}$ .

(e)

**Proposition 12** Si  $A$  et  $2D - A$  sont symétriques définies positives alors la méthode de Jacobi converge pour tout choix de  $x^{(0)}$ .

(f)

**Proposition 12** Si  $A$  et  $2D - A$  sont symétriques définies positives alors la méthode de Jacobi converge pour tout choix de  $x^{(0)}$ .

(g)

**Proposition 12** Si  $A$  et  $2D - A$  sont symétriques définies positives alors la méthode de Jacobi converge pour tout choix de  $x^{(0)}$ .

(h)

**Proposition 12** Si  $A$  et  $2D - A$  sont symétriques définies positives alors la méthode de Jacobi converge pour tout choix de  $x^{(0)}$ .

(i)

Figure 2: From top to bottom, (a) the original image 'Proposition', the recovered reflectance by (b) MSRetinex [40], (c) Variational Retinex [25], (d) Screened Poisson Equation [34], (e) PDE Retinex [29], (f) local laplacian model [32], (g) the local derivatives model [32], (h) the first proposed nonlocal laplacian model, (i) the second proposed non-local derivatives model

2- Un jeu de carte contient 32 cartes. On en prend 3 successivement, sans remise. De combien de façons peut opérer pour obtenir au moins un cœur ?

(a)

2- Un jeu de carte contient 32 cartes. On en prend 3 successivement, sans remise. De combien de façons peut opérer pour obtenir au moins un cœur ?

(b)

2- Un jeu de carte contient 32 cartes. On en prend 3 successivement, sans remise. De combien de façons peut opérer pour obtenir au moins un cœur ?

(c)

2- Un jeu de carte contient 32 cartes. On en prend 3 successivement, sans remise. De combien de façons peut opérer pour obtenir au moins un cœur ?

(d)

2- Un jeu de carte contient 32 cartes. On en prend 3 successivement, sans remise. De combien de façons peut opérer pour obtenir au moins un cœur ?

(e)

2- Un jeu de carte contient 32 cartes. On en prend 3 successivement, sans remise. De combien de façons peut opérer pour obtenir au moins un cœur ?

(f)

2- Un jeu de carte contient 32 cartes. On en prend 3 successivement, sans remise. De combien de façons peut opérer pour obtenir au moins un cœur ?

(g)

2- Un jeu de carte contient 32 cartes. On en prend 3 successivement, sans remise. De combien de façons peut opérer pour obtenir au moins un cœur ?

(h)

2- Un jeu de carte contient 32 cartes. On en prend 3 successivement, sans remise. De combien de façons peut opérer pour obtenir au moins un cœur ?

(i)

Figure 3: From top to bottom, (a) the original image 'Exercise', the recovered reflectance by (b) MSRetinex [40], (c) Variational Retinex [25], (d) Screened Poisson Equation [34], (e) PDE Retinex [29], (f) local laplacian model [32], (g) the local derivatives model [32], (h) the first proposed nonlocal laplacian model, (i) the second proposed nonlocal derivatives model

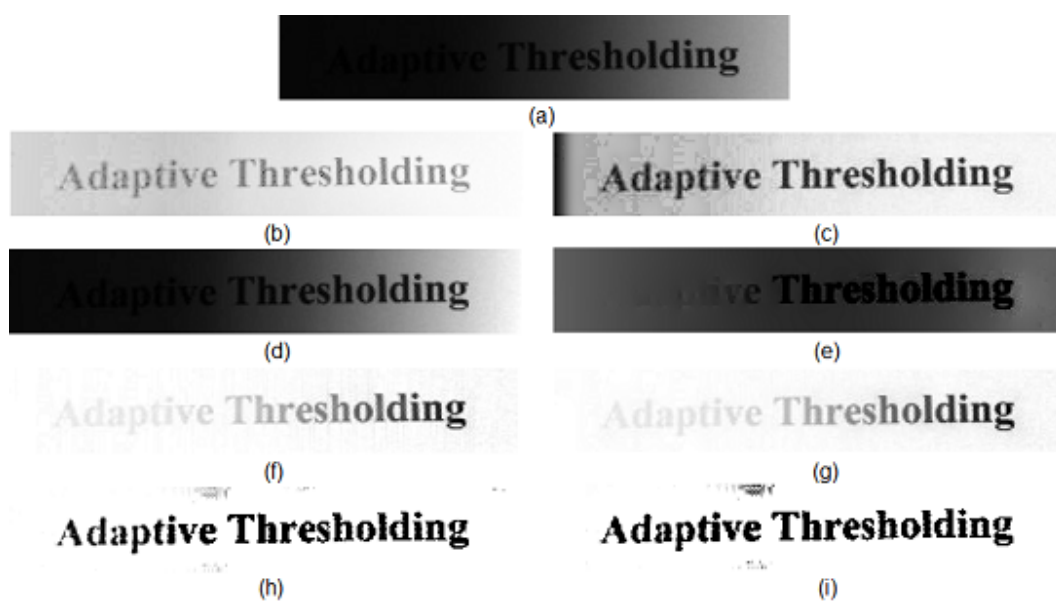


Figure 4: From top to bottom and from left to right, (a) the original image 'Phrase', the recovered reflectance by (b) MSRetinex [40], (c) Variational Retinex [25], (d) Screened Poisson Equation [34], (e) PDE Retinex [29], (f) local laplacian model [32], (g) the local derivatives model [32], (h) the first proposed nonlocal laplacian model, (i) the second proposed nonlocal derivatives model

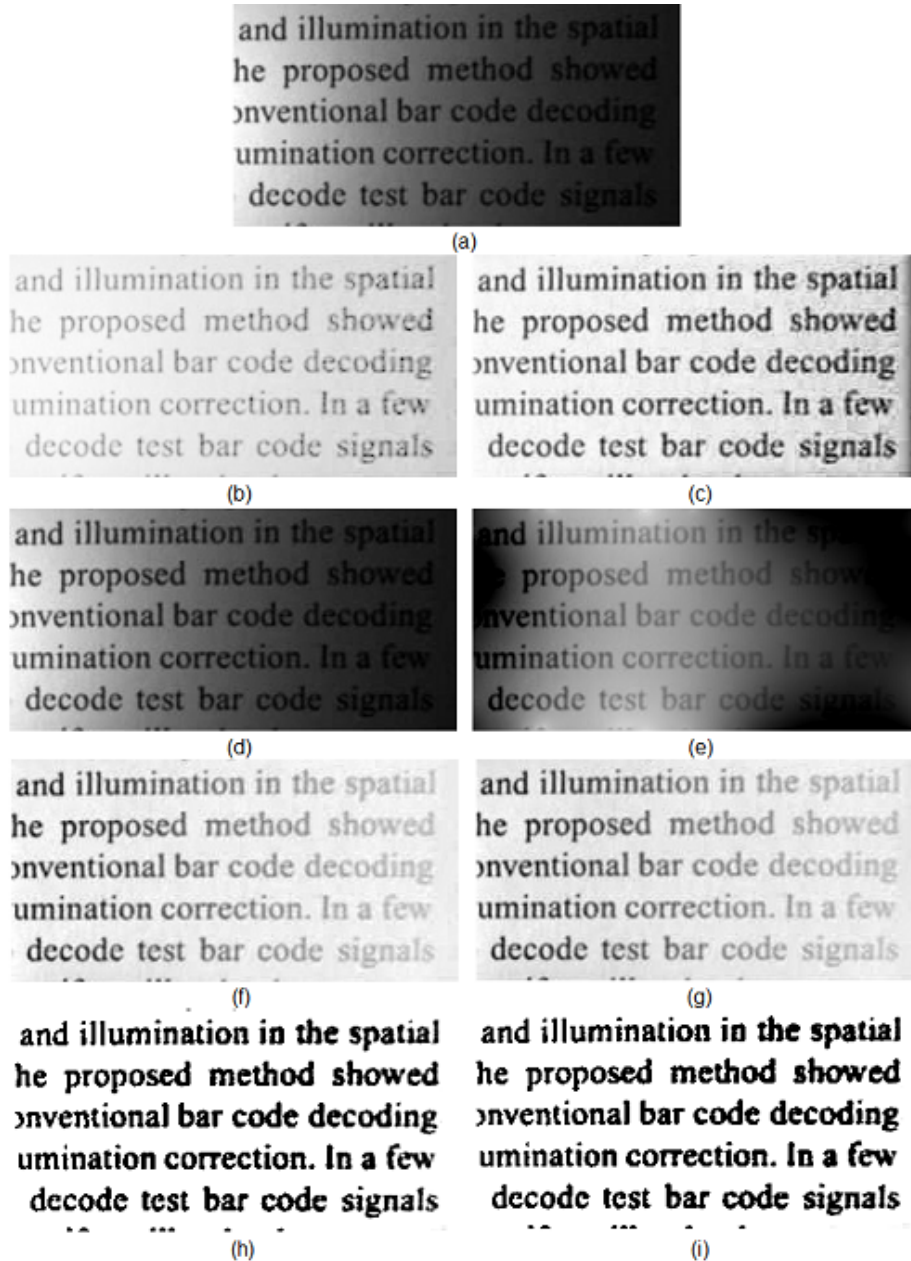


Figure 5: From top to bottom and from left to right, (a) the original image 'Text', the recovered reflectance by (b) MSRetinex [40], (c) Variational Retinex [25], (d) Screened Poisson Equation [34], (e) PDE Retinex [29], (f) local laplacian model [32], (g) the local derivatives model [32], (h) the first proposed nonlocal laplacian model, (i) the second proposed nonlocal derivatives model

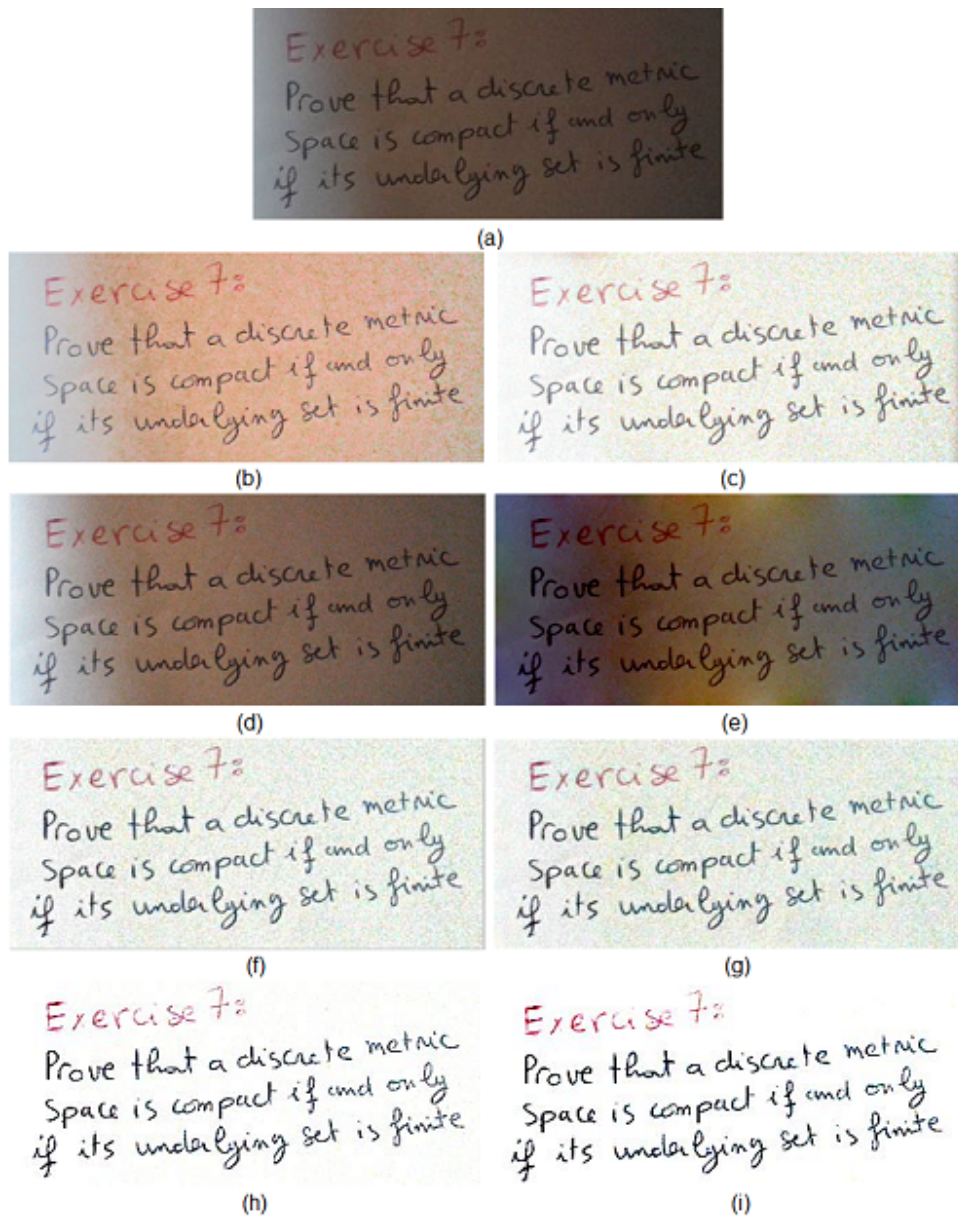


Figure 6: From top to bottom and from left to right, (a) the original image 'Exercise 7', the recovered reflectance by (b) MSRetinex [40], (c) Variational Retinex [25], (d) Screened Poisson Equation [34], (e) PDE Retinex [29], (f) local laplacian model [32], (g) the local derivatives model [32], (h) the first proposed nonlocal laplacian model, (i) the second proposed nonlocal derivatives model

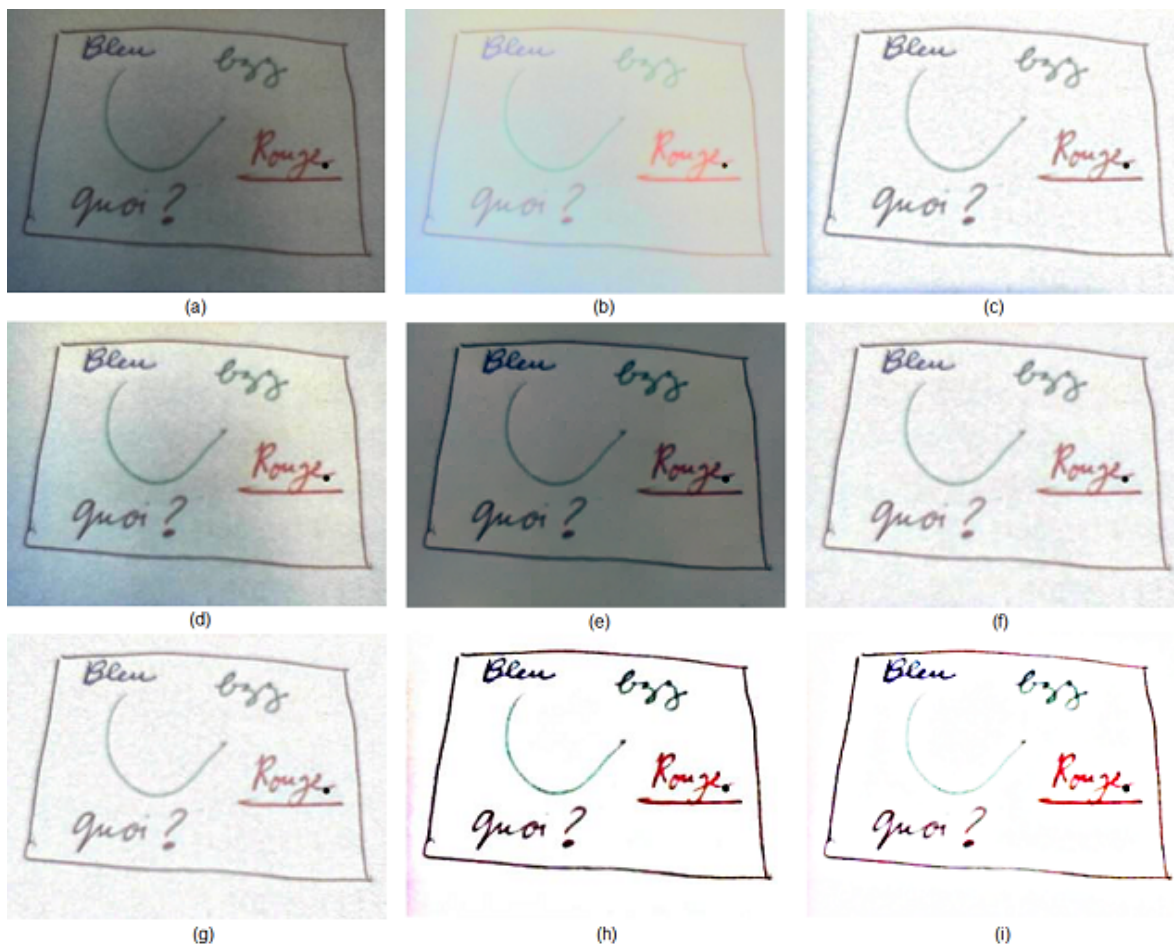


Figure 7: From top to bottom and from left to right, (a) the original image 'Board', the recovered reflectance by (b) MSRetinex [40], (c) Variational Retinex [25], (d) Screened Poisson Equation [34], (e) PDE Retinex [29], (f) local laplacian model [32], (g) the local derivatives model [32], (h) the first proposed nonlocal laplacian model, (i) the second proposed nonlocal derivatives model



Image	Method	FineReader %	OnlineOCR %	Tesseract %
Proposition	the original	72.11	77.88	0
	MSRetinex	82.69	95.19	0
	Var. Retinex	95.19	95.19	<b>82.69</b>
	Screened Poisson Equ	91.35	82.96	0
	PDE Retinex	0	0	0
	L.Laplacian Model	96.15	<b>98.08</b>	75
	L.Derivatives Model	96.15	<b>98.08</b>	<b>80.77</b>
	The proposed Model 1	<b>97.11</b>	<b>98.08</b>	75
	The proposed Model 2	<b>98.08</b>	<b>96.15</b>	76.92
Exercise	the original	0	0	0
	MSRetinex	76.67	97.5	0
	Var. Retinex	98.33	95.83	10
	Screened Poisson Equ	98.33	<b>100</b>	0
	PDE Retinex	0	0	0
	L.Laplacian Model	95.83	93.33	37.5
	L.Derivatives Model	93.33	95	40.83
	The proposed Model 1	<b>100</b>	<b>100</b>	<b>82.5</b>
	The proposed Model 2	<b>99.17</b>	<b>97.5</b>	<b>82.5</b>
Phrase	the original	0	0	0
	MSRetinex	95	<b>100</b>	0
	Var. Retinex	<b>100</b>	95	60
	Screened Poisson Equ	35	0	0
	PDE Retinex	0	60	0
	L.Laplacian Model	45	60	50
	L.Derivatives Model	50	60	55
	The proposed Model 1	<b>100</b>	<b>100</b>	<b>100</b>
	The proposed Model 2	<b>100</b>	<b>100</b>	<b>100</b>
Text	the original	39.2	62.4	0
	MSRetinex	92	95.2	43.2
	Var. Retinex	<b>99.19</b>	<b>100</b>	89.6
	Screened Poisson Equ	56.8	64.8	0
	PDE Retinex	18.4	31.2	0
	L.Laplacian Model	68.8	99.19	85.6
	L.Derivatives Model	68.8	99.19	86.4
	The proposed Model 1	<b>99.19</b>	<b>100</b>	<b>98.39</b>
	The proposed Model 2	<b>100</b>	<b>100</b>	<b>98.39</b>

Table 1: **OCR accuracy results**

## 6. Conclusion

In the present paper, an existence result for the local PDE's text enhancement model proposed in (6) was given, then, based on the nonlocal operators properties, two nonlocal models were proposed to estimate the reflectance image. Moreover, the two nonlocal algorithms are simple, easy to implement and give quite satisfactory results compared to some available methods, which gives confidence in the efficiency of our models. Beyond the two proposed nonlocal PDEs, we could also extend these two models to other PDEs with more regularity properties.

## References

- [1] Gilles Aubert and Pierre Kornprobst. *Mathematical problems in image processing: partial differential equations and the calculus of variations*, volume 147. Springer Science & Business Media, 2006.
- [2] M Bardi, MG Crandall, LC Evans, HM Soner, and PE Souganidis. Viscosity solutions and applications. lectures given at the 2nd cime session held in montecatini terme, june 12–20, 1995. edited by i. capuzzo dolcetta and pl lions. *Lecture Notes in Mathematics*, 1660.
- [3] Andrew Blake. On lightness computation in mondrian world. In *Central and peripheral mechanisms of colour vision*, pages 45–59. Springer, 1985.
- [4] Gavin Brelstaff and Andrew Blake. Computing lightness. *Pattern Recognition Letters*, 5(2):129–138, 1987.
- [5] Antoni Buades, Bartomeu Coll, and J-M Morel. A non-local algorithm for image denoising. In *Computer Vision and Pattern Recognition, 2005. CVPR 2005. IEEE Computer Society Conference on*, volume 2, pages 60–65. IEEE, 2005.
- [6] Antoni Buades, Bartomeu Coll, and Jean-Michel Morel. Nonlocal image and movie denoising. *International journal of computer vision*, 76(2):123–139, 2008.
- [7] Gulcin Caner and Ismail Haritaoglu. Shape-dna: Effective character restoration and enhancement for arabic text documents. In *Pattern Recognition (ICPR), 2010 20th International Conference on*, pages 2053–2056. IEEE, 2010.

- [8] Michael G Crandall, Hitoshi Ishii, and Pierre-Louis Lions. User’s guide to viscosity solutions of second order partial differential equations. *Bulletin of the American Mathematical Society*, 27(1):1–67, 1992.
- [9] Alexei A Efros and Thomas K Leung. Texture synthesis by non-parametric sampling. In *Computer Vision, 1999. The Proceedings of the Seventh IEEE International Conference on*, volume 2, pages 1033–1038. IEEE, 1999.
- [10] Chun-Nian Fan and Fu-Yan Zhang. Homomorphic filtering based illumination normalization method for face recognition. *Pattern Recognition Letters*, 32(10):1468–1479, 2011.
- [11] Ya-Ru Fan, Ting-Zhu Huang, Tian-Hui Ma, and Xi-Le Zhao. Cartoon–texture image decomposition via non-convex low-rank texture regularization. *Journal of the Franklin Institute*, 354(7):3170–3187, 2017.
- [12] R Fries and J Modestino. Image enhancement by stochastic homomorphic filtering. *IEEE Transactions on Acoustics, Speech, and Signal Processing*, 27(6):625–637, 1979.
- [13] R Fries and J Modestino. Image enhancement by stochastic homomorphic filtering. *IEEE Transactions on Acoustics, Speech, and Signal Processing*, 27(6):625–637, 1979.
- [14] Marius Ghergu and Vicentiu Radulescu. *Nonlinear PDEs: Mathematical models in biology, chemistry and population genetics*. Springer Science & Business Media, 2011.
- [15] Yoshikazu Giga. *Surface evolution equations: A level set approach*, volume 99. Springer Science & Business Media, 2006.
- [16] Guy Gilboa and Stanley Osher. Nonlocal operators with applications to image processing. *Multiscale Modeling & Simulation*, 7(3):1005–1028, 2008.
- [17] Pelin Gorgel, Ahmet Sertbas, and Osman N Ucan. A wavelet-based mammographic image denoising and enhancement with homomorphic filtering. *Journal of medical systems*, 34(6):993–1002, 2010.
- [18] Berthold Horn. *Robot vision*. MIT press, 1986.

- [19] Berthold KP Horn. Determining lightness from an image. *Computer graphics and image processing*, 3(4):277–299, 1974.
- [20] Yali Huang, Yuehua Gao, Hong Wang, Dongmei Hao, Jinhui Zhao, and Zhen Zhao. Enhancement of ultrasonic image based on the multi-scale retinex theory. In *Recent Advances in Computer Science and Information Engineering*, pages 115–120. Springer, 2012.
- [21] Hitoshi Ishii and Moto-Hiko Sato. Nonlinear oblique derivative problems for singular degenerate parabolic equations on a general domain. *Nonlinear Analysis: Theory, Methods & Applications*, 57(7):1077–1098, 2004.
- [22] Wei W Cindy Jiang. Thresholding and enhancement of text images for character recognition. In *Acoustics, Speech, and Signal Processing, 1995. ICASSP-95., 1995 International Conference on*, volume 4, pages 2395–2398. IEEE, 1995.
- [23] Wei W Cindy Jiang. Thresholding and enhancement of text images for character recognition. In *Acoustics, Speech, and Signal Processing, 1995. ICASSP-95., 1995 International Conference on*, volume 4, pages 2395–2398. IEEE, 1995.
- [24] Daniel J Jobson, Zia-ur Rahman, and Glenn A Woodell. A multiscale retinex for bridging the gap between color images and the human observation of scenes. *IEEE Transactions on Image processing*, 6(7):965–976, 1997.
- [25] Ron Kimmel, Michael Elad, Doron Shaked, Renato Keshet, and Irwin Sobel. A variational framework for retinex. *International Journal of computer vision*, 52(1):7–23, 2003.
- [26] Edwin H Land. The retinex theory of color vision. *Scientific American*, 237(6):108–129, 1977.
- [27] Edwin H Land and John J McCann. Lightness and retinex theory. *Josa*, 61(1):1–11, 1971.
- [28] Jingwei Liang and Xiaoqun Zhang. Retinex by higher order total variation  $l^1$  decomposition. *Journal of Mathematical Imaging and Vision*, 52(3):345–355, 2015.

- [29] Nicolas Limare, Ana Belén Petro, Catalina Sbert, and Jean-Michel Morel. Retinex poisson equation: a model for color perception. *Image Processing On Line*, 1:39–50, 2011.
- [30] Guowen Ma and Jinfeng Yang. Shadow removal using retinex theory. In *Intelligent Visual Surveillance (IVS), 2011 Third Chinese Conference on*, pages 25–28. IEEE, 2011.
- [31] Wenye Ma and Stanley Osher. A tv bregman iterative model of retinex theory. *Ucla Cam Report*, pages 10–13, 2010.
- [32] Zouhir Mahani, Jalal Zahid, Sahar Saoud, Mohammed El Rhabi, and Abdelilah Hakim. Text enhancement by pde’s based methods. *Image and Signal Processing*, pages 65–76, 2012.
- [33] John McCann. Lessons learned from mondrians applied to real images and color gamuts. In *Color and imaging conference*, volume 1999, pages 1–8. Society for Imaging Science and Technology, 1999.
- [34] Jean-Michel Morel, Ana-Belen Petro, and Catalina Sbert. Screened poisson equation for image contrast enhancement. *Image Processing On Line*, 4:16–29, 2014.
- [35] Michael K Ng and Wei Wang. A total variation model for retinex. *SIAM Journal on Imaging Sciences*, 4(1):345–365, 2011.
- [36] Uche Nnolim and Peter Lee. Homomorphic filtering of colour images using a spatial filter kernel in the hsi colour space. In *Instrumentation and Measurement Technology Conference Proceedings, 2008. IMTC 2008. IEEE*, pages 1738–1743. IEEE, 2008.
- [37] A van Oppenheim, Ronald Schafer, and Thomas Stockham. Nonlinear filtering of multiplied and convolved signals. *IEEE transactions on audio and electroacoustics*, 16(3):437–466, 1968.
- [38] A. Pazy. Semigroups of linear operators and applications to partial differential equations. 1983.
- [39] Soo-Chang Pei, Mary Tzeng, and Yu-Zhe Hsiao. Enhancement of uneven lighting text image using line-based empirical mode decomposition. In *Acoustics, Speech and Signal Processing (ICASSP), 2011 IEEE International Conference on*, pages 1249–1252. IEEE, 2011.

- [40] Ana Belén Petro, Catalina Sbert, and Jean-Michel Morel. Multiscale retinex. *Image Processing On Line*, pages 71–88, 2014.
- [41] Aishwarya Visvanathan, T Chattopadhyay, and Ujjwal Bhattacharya. Enhancement of camera captured text images with specular reflection. In *Computer Vision, Pattern Recognition, Image Processing and Graphics (NCVPRIPG), 2013 Fourth National Conference on*, pages 1–4. IEEE, 2013.
- [42] Guoxin Xue, Pei Xue, and Qiang Liu. A method to improve the retinex image enhancement algorithm based on wavelet theory. In *Computational Intelligence and Design (ISCID), 2010 International Symposium on*, volume 1, pages 182–185. IEEE, 2010.
- [43] Leonid Yaroslavsky. *Digital picture processing: an introduction*, volume 9. Springer Science & Business Media, 2012.

#### **Conflict of interest**

The authors declare that they have no conflict of interest.